

# NUMERICAL STUDY OF THE DELTA II POLARIZING UNDULATOR FOR LCLS II\*

K. Tian<sup>†</sup>, H.-D. Nuhn

SLAC National Accelerator Laboratory, Menlo Park, CA, USA

## Abstract

The Delta undulator has been operated successfully in LCLS with full control of the polarization mode and  $K$  value of the device. In LCLS II, a new Delta II undulator will be based on a similar design but with some differences. In this paper, we will present numerical simulation results that provide guidance to choose the geometric shape of the magnet poles and define the required tolerance for assembling the undulator magnets.

## INTRODUCTION

The Delta II undulator is 3.28 m long with a period length of 44 mm. Unlike the fixed magnet gap of the Delta undulator [1–3] for LCLS, the  $K$  value of the Delta II undulator will be adjusted by varying the gap of the device, which causes some challenges in controlling mechanical tolerances and alignment errors. The Delta undulator used round shape tips for the magnet blocks. However, if a flat shaped magnet tip can also meet the field requirement, it can be beneficial to the development of the new device due to its simplicity in obtaining high precision of production. To help in determining the final design of the magnet block of the Delta II undulator, we compare the  $K$  values of the Delta II undulator using several different magnet tip shapes, including a round shape, a flat shape, and two triangular shapes, as show in Fig. 1, where only one of the triangular poles is shown.

In an ideal undulator, the  $K$  parameter is constant along the device axis. However, after the assembly of the 4 quadrants of the original LCLS Delta undulator, systematic errors in the radial position of the magnet arrays along the undulator axis were observed [4, 5]. In order to establish tolerances, we will consider two types of error in the placement of the magnet row of the Delta II undulator: a quadrant bow and a quadrant taper. In Radia [6] simulations, we add these errors to the insertion device model for solving the magnet fields with these effects.

## MAGNET TIP GEOMETRY

The magnet blocks are generated in Radia using the built-in function radObjThckPgn, and then form the full assembly of four rows of magnet arrays. Two criteria have been used to evaluate the performance of the Delta II undulator with different tip shapes of the magnet block: first, the  $K$  value at the minimum gap is required to be larger than 5.14, set by the parameters of the LCLS II SXR undulator; second, the transverse position dependence of  $K$  near the beam axis

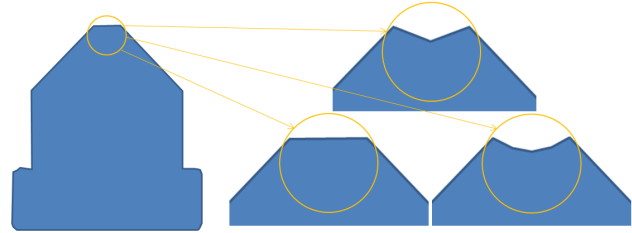


Figure 1: Magnet tip geometries used in the simulations.

needs to be as small as possible ( $K$  flatness). For studying the second criterion, we calculate the transverse  $K$  values along both  $x$  and  $y$  axes with an offset of 0.03 mm, 0.1 mm, 0.2 mm, 0.3 mm, 0.5 mm, and 1 mm, respectively.

The undulator  $K$  is derived from the first derivative of the Phase Integral ( $PI$ ),  $dPI/dz$ , electron mass  $m_e$  and charge  $e$ , and speed of light  $c$  using the following formula with the bracket denoting for taking arithmetic mean:

$$K = \frac{e\sqrt{2} \langle dPI/dz \rangle}{m_e c}, \quad (1)$$

where  $PI$  is defined by:

$$PI(z) = \int_0^z \left[ \left( \int_0^{\bar{z}} B_x(\bar{z}) d\bar{z} \right)^2 + \left( \int_0^{\bar{z}} B_y(\bar{z}) d\bar{z} \right)^2 \right] d\bar{z}, \quad (2)$$

and is evaluated from  $B_x$  and  $B_y$  along a line parallel to the beam axis at different offsets. For this study, we use an undulator model consisting of 4 regular periods and the end pieces, making the model much shorter than the actual device. Therefore, to overcome the influence of the fields from end pieces, we adopt a moving window averaging technique in calculating the  $PI$  and the mean of the first derivative of  $PI$ , for only one core period around the center of the device.

The results for the circular polarization at minimum gap are shown in Fig. 2. The legend in Fig. 2(b) can be used to correlate the results with the shapes of the magnet tips. Results in all cases exceed the required  $K$  value of 5.14. The device simulated with round tips has the largest  $K$  values, and the design with flat tips possesses the smallest  $K$  values, while the  $K$  values for the two cases with triangular tips fall in between. The on axis  $K$  value for a round tip is 5.62 in comparison with the  $K$  value of 5.54 for a flat tip, or about 1.4% improvement. Therefore the gain of  $K$  is moderate. To compare the flatness of  $K$ , in Fig. 2(b) and (d), we plot the relative difference of  $K$ , in percent, from the beam axis as a function of the offset. The results from different tip shapes are very similar. On both, the  $x$  and the  $y$  axis, the flatness crosses 0.01% at about 150  $\mu\text{m}$  from the origin.

\* Work supported by US Department of Energy Contract DE-AC03-76SF00515.

<sup>†</sup> email address: ktian@slac.stanford.edu

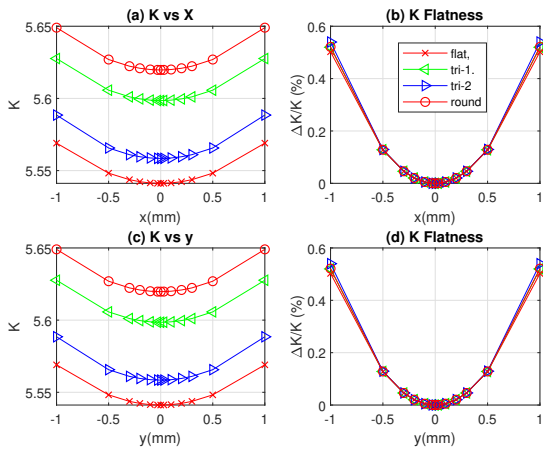


Figure 2: Simulation results for circular polarization mode at minimum gap.

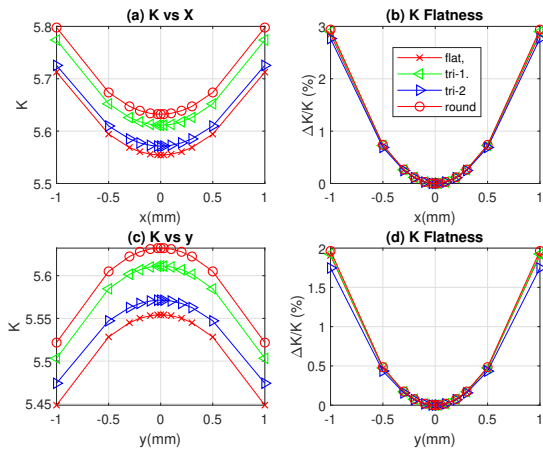


Figure 3: Simulation results for linear polarization at minimum gap.

The simulation results for the linear polarization mode in Fig. 3 are mostly similar to those for the circular polarization mode except that, in Fig. 3(c),  $K$  decreases with  $y$  in contrast to the opposite trends in Fig. 2(c). Another thing worth noting is that the  $K$  flatness for the linear polarization is a bit worse than that for the circular polarization. On both  $x$  and  $y$  axis, it exceeds 0.01% with an offset less than 100  $\mu\text{m}$ .

## MECHANICAL TOLERANCES

As shown in Fig. 4, for quadrant bow, assuming that both end blocks have zero radial offsets from the nominal position, the maximum offset of the magnet pole,  $r_{max}^b$ , occurs at the center of the ID; for quadrant taper, we assume zero offset for the first upstream block and the maximum offset  $r_{max}^t$  at the downstream end. In the Radia model, we add these errors for solving the magnetic fields with these effects. In a PC with 64 GB memory, it was possible to simulate a Delta II model with 70 core periods, but the computing time is usually more than 24 hours. Therefore, for the tolerance study, we chose

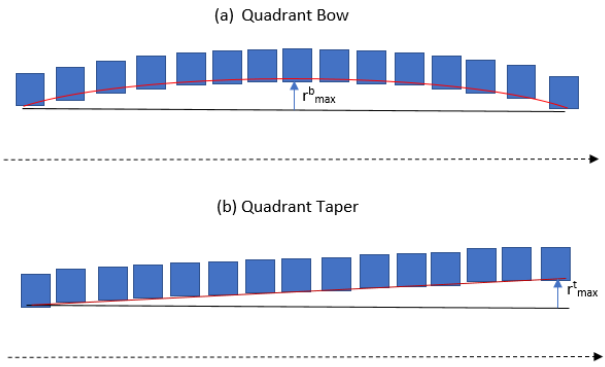


Figure 4: Systematic errors of the magnet poles: (a) Bow errors; (b) Taper errors.

a model with 50 core periods with a shorter computing time of several hours. To characterize the effects of different quadrant errors, we evaluated the phase shake,  $\sigma_{d\phi}$ , the standard deviation of the phase errors and the undulator efficiency,  $\chi$ , which will be defined in the following.

## Phase Shake

Besides the core magnet blocks, each magnet row of the Delta II undulator contains field matching magnet blocks at both ends (7/8 period). In order to evaluate the effects of quadrant errors on phase errors and phase shake, it is desirable to exclude the end effects. After examining the on-axis magnetic field, it appears that the magnet field of the first and last 2-4 core periods is still affected by the end effects. After comparing the calculated results for phase shake from simulation with that from the analytical formula[4] with different numbers of core periods excluded from both ends, it showed that, after taking out 4 core periods at each end, the phase errors derived from numerical simulation are nearly identical to the analytical results. Therefore, we will calculate the phase errors after excluding the magnetic field from the first and last four core periods. We will follow the same approach for a numerical model with more than 50 core periods.

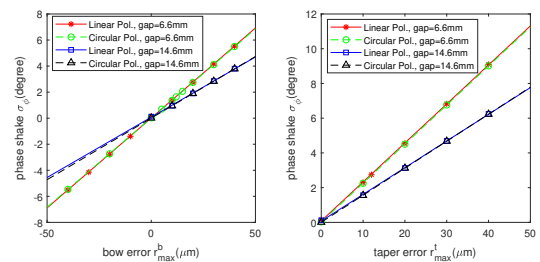


Figure 5: Simulation results of the phase shake for Delta II undulator with bow errors (left) or taper errors (right).

The phase shake is the standard deviation of the phase errors, therefore, even when the phase errors show opposite signs, the calculated values of phase shake always have the same positive sign and are actually roughly equal for

Content from this work may be used under the terms of the CC BY 3.0 licence (© 2019). Any distribution of this work must maintain attribution to the author(s), title of the work, publisher, and DOI

these two particular cases. For the convenience of the fitting analysis, we arbitrarily choose to define the phase shake for the undulator model with negative row errors, i.e.  $r_{max}^b$  or  $r_{max}^t < 0$ , to have negative phase shake. This definition helps in fitting the data with a straight line. In fact, the linear relationship between the maximum row errors and the phase shake applies to all the numerical configuration we set up for the Delta II undulators.

Simulation results for all scenarios are shown in Fig. 5. All four rows have the same quadrant errors in each simulation. Several observations can be made from the comparison of the results in Fig. 5. First, both types of row errors have larger effects on the phase shake at the smaller gap compared to the larger gap, which is intuitive because the same geometric distortion on the magnet rows should introduce more perturbations when the field strength is larger. Furthermore, the taper errors introduce more phase shake than the bow errors. For example, the taper error with maximum amplitude of  $40 \mu\text{m}$  leads to a phase shake of a bit over  $8^\circ$  vs. less than  $6^\circ$  for the bow error with the same maximum amplitude for an ID at 6.6 mm gap. Lastly, one can note that the polarization mode of the device plays a negligible role here.

### Undulator Efficiency

Delta II undulators will be placed after the micro-bunching undulators and be operated in afterburner mode[3]. As a result, the lasing condition of the Delta II undulator is dependent on the micro-bunching of the electron beam. From the operating experience with the Delta undulator in LCLS, the output laser power  $P$  appears to be a narrow band resonance with respect to the  $K$  parameter of the undulator:

$$P = P_{max} e^{-\frac{(K-K_r)^2}{2\sigma_K^2}}, \quad (3)$$

where  $P_{max}$  represents the laser power at resonance,  $\sigma_K = 0.00982$  from LCLS data, and  $K_r$  is the resonance undulator parameter determined by the micro-bunching of the electron beam. When the undulator  $K$  varies with longitudinal position, we can define the undulator efficiency,  $\chi$ , as the following:

$$\chi = \frac{\int P dz}{\int P_{max} dz} = \frac{\int e^{-\frac{(K(z)-K_r)^2}{2\sigma_K^2}} dz}{\int 1 \cdot dz}. \quad (4)$$

During the operation of the Delta II undulator, the maximum undulator efficiency can be obtained by adjusting the undulator gap. In this study, we want to learn, at a fixed gap, the change of optimum undulator efficiency due to row errors. For each simulation in Radia, the on-axis magnetic field is sampled at a step size of  $84.4 \mu\text{m}$ , or 535 samples per undulator period. Therefore, for a given undulator model with certain row errors,  $K(z)$  can be calculated at each grid point and we can also numerically find the value of  $K_r$  that makes  $\chi$  maximum. We define the corresponding  $K_r$  as effective undulator parameter  $K_{eff}$  and the  $\chi$  as optimum

undulator efficiency  $\chi_{opt}$  for this device. Obviously, for an ideal undulator with constant  $K$  along  $z$ ,  $\chi_{opt}=1$ , otherwise,  $\chi_{opt}<1$ . However, due to numerical noise and end effects, the undulator  $K$  of a device without row errors still varies by about 0.08%, which is enough to significantly reduce the  $\chi_{opt}$ . We believe that the variation of  $K$  can be reduced or eliminated by adopting certain processing techniques. But one should note that in the actual process of undulator tuning, local perturbation to individual poles may introduce similar effects on the undulator performance like the numerical noise in the simulations. In this paper, we are trying to determine the tolerance on bow/taper errors, so we want to focus on their effects by normalizing the undulator efficiency of the device with errors to that of the same device without errors. Hence, we define the relative undulator efficiency:

$$\chi_r = \frac{\chi_{opt}}{\chi_{opt}(r_{max}^b = r_{max}^t = 0)}. \quad (5)$$

The effects of row errors on the relative undulator efficiency  $\chi_r$  are shown in Fig. 6. Similar to the results for phase shake, the reduction of undulator efficiency due to the row errors depends more on the magnet gap of the device than the polarization. In order to maintain a high efficiency, one has to keep tight control on the row errors. For example, at minimum gap, it will be necessary to have a tolerance less than  $15 \mu\text{m}$  for an undulator efficiency over 90%. On the other hand, for a mechanical tolerance of  $40 \mu\text{m}$ , the undulator efficiency drops to 50-60% depending on the types of row errors.

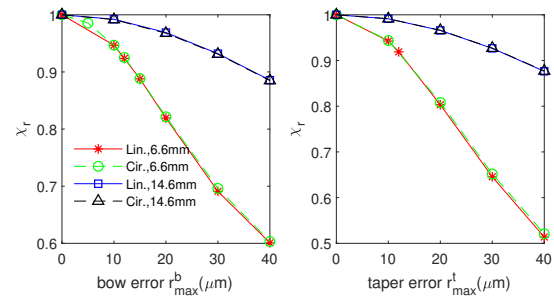


Figure 6: Simulation results of the undulator efficiency for Delta II undulator with bow errors (left) or taper errors (right).

## CONCLUSION

We have developed numerical routines to study the performance of the Delta II undulator with different tip geometry and quadrant row errors. Simulation results suggest that the flat shape design of the magnet tip should be sufficient to meet the operational requirement. It also appears that the quadrant errors have more pronounced effects on the undulator efficiency than the phase shake.

## ACKNOWLEDGEMENTS

We want to thanks O. Choubar for useful discussions.

## REFERENCES

- [1] A. B. Temnykh, "Delta undulator for Cornell energy recovery linac," *Phys. Rev. Accel. Beams*, vol. 11, p. 120702, 2019.
- [2] H.-D. Nuhn *et al.*, "R&D towards a delta-type undulator for the LCLS," in *Proceedings of the 35th International Free Electron Laser Conference*, New York, NY, USA: JACoW, 2013, p. 348.
- [3] H.-D. Nuhn *et al.*, "Commissioning of the delta polarizing undulator at LCLS," in *Proceedings of the 37th International Free Electron Laser Conference*, Daejeon, Korea: JACoW, 2015, paper TUPS052, p.757.
- [4] Z. Wolf, "Effect of quadrant bow on delta undulator phase errors," in *LCLS-TN-15-1*, 2015.
- [5] Z. Wolf, "Effect of quadrant taper on delta undulator phase errors," in *LCLS-TN-15-2*, 2015.
- [6] P. Elleaume, O. Chubar, and J. Chavanne, "Computing 3D magnetic field from insertion devices," in *Proceedings of the 1997 Particle Accelerator Conference*, Vancouver, B.C., Canada: IEEE, 1997, p. 3509.